

# PRECISION CRYSTAL CALORIMETRY IN HIGH ENERGY PHYSICS

Ren-yuan Zhu

*Physics Department, California Institute of Technology, Pasadena, CA 91125, U.S.A.*

Crystal Calorimetry is widely used in high energy physics because of its precision. Recent development in crystal technology identified two key issues to reach and maintain crystal precision: light response uniformity and calibration *in situ*. Crystal radiation damage is understood. While the damage in alkali halides is found to be caused by the oxygen/hydroxyl contamination, it is the structure defects, such as oxygen vacancies, cause damage in oxides.

## I. INTRODUCTION

Total absorption shower counters made of inorganic scintillating crystals have been known for decades for their superb energy resolution and detection efficiency. In high energy and nuclear physics, large arrays of scintillating crystals have been assembled for precision measurements of photons and electrons. Recently, several crystal calorimeters have been designed and are under construction for the next generation of high energy physics experiment. Table I summarizes design parameters for these crystal calorimeters. One notes that each of these calorimeters requires several cubic meters of high quality crystals.

CsI(Tl) crystals are known to have high light yield, so was chosen by two B Factory experiments where low noise is essential for low end of energy reach. PbWO<sub>4</sub> crystals are distinguished with their high density, short radiation length and small Molière radius, so was chosen by CMS experiment to construct a compact crystal calorimeter of 25 radiation length. The low light yield of PbWO<sub>4</sub> crystals can be overcome by gains of the photo-detector, such as PMTs and avalanche photodiodes (APD). The unique physics capability of crystal calorimetry is the result of its superb energy resolution, hermetic coverage and fine granularity [1]. Recently designed crystal calorimeters, however, face a new challenge: radiation damage caused by increased center of mass energy and luminosity. While dose rate is expected to be a few rad per day for CsI(Tl) crystals at two B Factories, it would reach 15 to 600 rad per hour for PbWO<sub>4</sub> crystals at LHC.

This paper discusses two key issues related to precision of crystal calorimetry *in situ*, and cause and cure of radiation damage in crystals. Light response uniformity and calibration *in situ* are discussed in Sections II and III. Effect of radiation damage is elaborated in Section IV. Section V discusses damage mechanism for alkali halides, such as BaF<sub>2</sub> and CsI, and oxides, such as bithmuth gemanade (Bi<sub>4</sub>Ge<sub>3</sub>O<sub>12</sub>, BGO) and PbWO<sub>4</sub>. Finally, a brief summary is given in Section VI.

All measurements, except specified otherwise, were carried out at Caltech with samples from Beijing Glass Research Institute (BGRI), Bogoroditsk Techno-Chemical Plant (BTCP), Khar'kov and Shanghai Institute of Ceramics (SIC).

TABLE I. Parameters of Recently Designed Crystal Calorimeters

| Experiment                       | KTeV            | <i>BaBar</i>    | BELLE           | CMS               |
|----------------------------------|-----------------|-----------------|-----------------|-------------------|
| Laboratory                       | FNAL            | SLAC            | KEK             | CERN              |
| Crystal Type                     | CsI             | CsI(Tl)         | CsI(Tl)         | PbWO <sub>4</sub> |
| B-Field (T)                      | -               | 1.5             | 1.0             | 4.0               |
| Inner Radius (m)                 | -               | 1.0             | 1.25            | 1.29              |
| Number of Crystals               | 3,300           | 6,580           | 8,800           | 83,300            |
| Crystal Depth (X <sub>0</sub> )  | 27              | 16 to 17.5      | 16.2            | 25                |
| Crystal Volume (m <sup>3</sup> ) | 2               | 5.9             | 9.5             | 11                |
| Light Output (p.e./MeV)          | 40              | 5,000           | 5,000           | 2                 |
| Photosensor                      | PMT             | Si PD           | Si PD           | APD <sup>a</sup>  |
| Gain of Photosensor              | 4,000           | 1               | 1               | 50                |
| Noise per Channel (MeV)          | small           | 0.15            | 0.2             | 30                |
| Dynamic Range                    | 10 <sup>4</sup> | 10 <sup>4</sup> | 10 <sup>4</sup> | 10 <sup>5</sup>   |

<sup>a</sup>Avalanche photodiode.

## II. CRYSTAL LIGHT RESPONSE UNIFORMITY

GEANT simulation shows that an adequate light response uniformity profile is a key to precision of a crystal calorimeter.

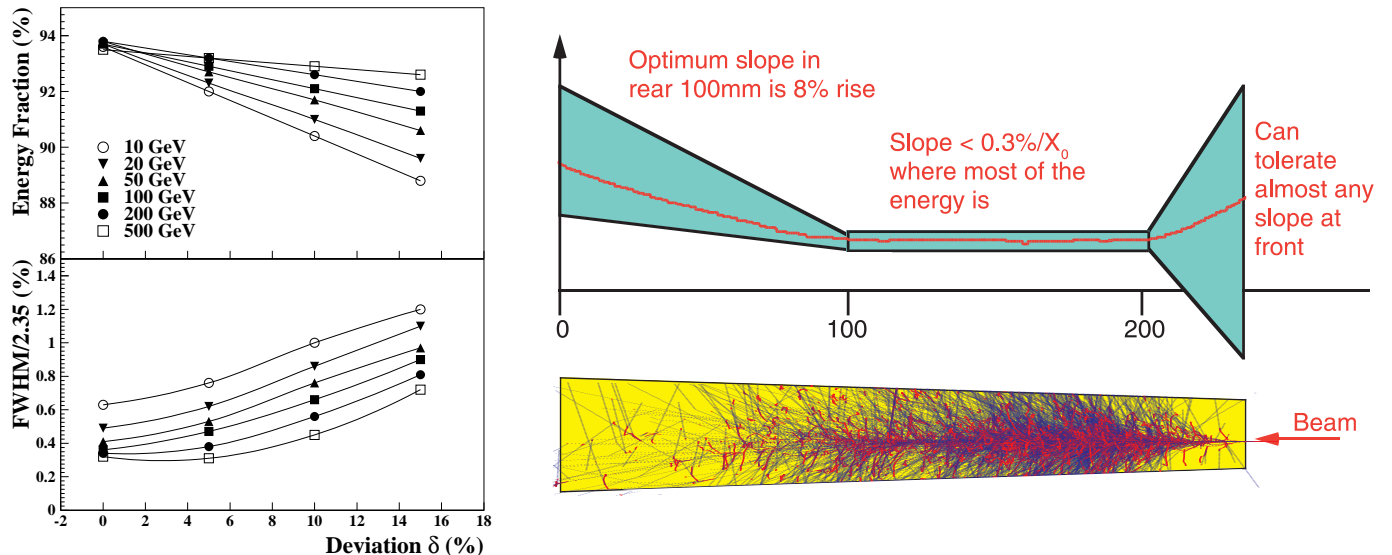


FIG. 1. Left: Effect of light response uniformity predicted by a GEANT simulation [2]. Right: Specification of light response uniformity profile for CMS PbWO<sub>4</sub> crystals [3].

The left side of Figure 1 [2] shows a GEANT prediction of energy fraction (top) and the intrinsic resolution (bottom) calculated by summing the energies deposited in a  $3 \times 3$  sub-array, consisting of tapered BaF<sub>2</sub> crystals of 25 radiation length, as a function of the light response uniformity. In this simulation, light response ( $y$ ) of the crystal was parametrized as a normalized linear function:

$$\frac{y}{y_{mid}} = 1 + \delta(x/x_{mid} - 1), \quad (1)$$

where  $y_{mid}$  represents light response at the middle of the crystal,  $\delta$  represents deviation of light response uniformity, and  $x$  is the distance from the small (front) end of tapered crystal.

While changes of amplitude of light output can be inter-calibrated, the loss of the energy resolution, caused by degradation of light response uniformity is not recoverable. To preserve crystal's intrinsic energy resolution light response uniformity thus must be kept within tolerance. According to above simulation, the  $\delta$  value is required to be less than 5% so that its contribution to the constant term of the energy resolution is less than 0.5%. A recent GEANT simulation for CMS PbWO<sub>4</sub> crystals confirmed this conclusion. The right side of Figure 1 [3] shows specification of CMS PbWO<sub>4</sub> uniformity profile. While the slope at the front  $3 X_0$  is not restricted, it must be kept within  $0.3\%/X_0$  in the middle  $10 X_0$ , and it is required to have a positive value of 8% in the back  $12 X_0$ , so that rear leakage at high energies can be compensated.

By using PbWO<sub>4</sub> crystals tuned according to this specification, an energy resolution of  $\frac{\delta E}{E} = \frac{4.1\%}{\sqrt{E}} \oplus 0.37\% \oplus 0.15/E$  was achieved in CMS test beam at CERN using current production PbWO<sub>4</sub> crystals with Si APD of 25 mm<sup>2</sup> [4]. Figure 2 shows the distributions of stochastic (left) and constant (middle) terms of energy resolution, and 0.45% energy resolution reconstructed in  $3 \times 3$  PbWO<sub>4</sub> crystals for 280 GeV electrons (right). This 4.1% stochastic term will be reduced to 3% by using two APDs instead of one in final design [5]. Note, this constant term of 0.37% achieved does not include uncertainties of calibration *in situ*.

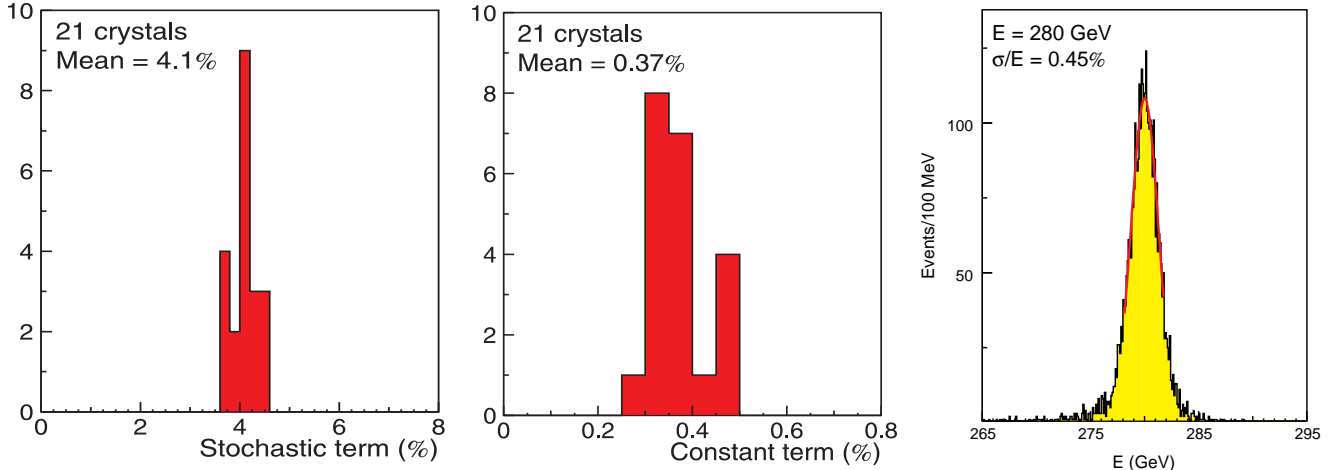


FIG. 2. Stochastic (Left) and constant (Middle) terms of energy resolution and 280 GeV electron signals (Right) obtained in CERN beam test.

### III. PRECISION CALIBRATION *IN SITU*

Precision calibration is the key factor in maintaining the crystal calorimetry precision *in situ*. Although all individual cells of a crystal calorimeter may be calibrated in a test beam at several different energies to provide a set of initial calibration constants before installation, the change in response over time differs from one calorimeter element (crystal, photo detector, readout chain) to the next. The left plot in Figure 3 shows BGO aging as a function of time of operation for two half barrels and two endcaps [6]. Inter-calibrations *in situ* therefore are required to track down the evolution of each channel independently.

Calibration *in situ* is most commonly achieved by using physics processes produced by beam, such as electrons or photons of known energy, electron or photon pairs reconstructible to a known invariant mass,  $E/p$  of electrons with momentum measured, and energy of minimum ionizing particles with known path length. Low energy  $\gamma$ -rays from radioactive sources or from radiative capture reactions are often used as a low energy calibration source. This is particularly important for those crystal calorimeters where physics processes do not occur at a high enough rate for a frequent calibration, such as L3 BGO [7]. Finally, a light pulser system is a useful tool to monitor the light collection in a crystal and the readout response. As discussed in Section IV, it can also serve as inter-calibration *in situ*, if the scintillation mechanism of crystals is not damaged.

Because of limited statistics of physics processes, L3 experiment uses a Radiofrequency Quadrupole (RFQ) based accelerator system for BGO crystal calibration. The 17.6 MeV  $\gamma$ -rays from a radiative capture reactions



is used as calibration source, which was produced by bombarding a Li target mounted inside the calorimeter with a proton beam. Shown in the middle of Figure 3 is the installation of RFQ calibration system in L3 detector. Combining with Bhabha events, the RFQ system provides sub percent calibration *in situ*, as shown in the right plot of Figure 3 [6].

For recently designed crystal calorimeters listed in Table I, KTeV uses  $E/p$  of electrons from  $K_L \rightarrow \pi^+ e^- \nu$ , *BaBar* and *BELLE* will use electrons from Bhabha scattering, and CMS will use  $E/p$  from electrons and  $Z \rightarrow e^+ e^-$  mass reconstruction. In addition, *BaBar* also uses 6.13 MeV  $\gamma$ -rays from a meta stable state of  ${}^{16}\text{O}$  with  $t_{1/2}$  of 7 sec, which is produced by circulating a fluorine containing fluid through a neutron source, and CMS also uses a light monitoring system to catch change of light collection in  $\text{PbWO}_4$  crystals *in situ*. By using  $E/p$  calibration, the KTeV CsI calorimeter has achieved a 0.6% resolution for electrons with energy larger than 20 GeV, indicating an accuracy of better than 0.5% is achieved in calibration *in situ* [8]. The goal of CMS experiment is to calibrate  $\text{PbWO}_4$  calorimeter to a similar or better level by using physics processes combined with light monitoring.

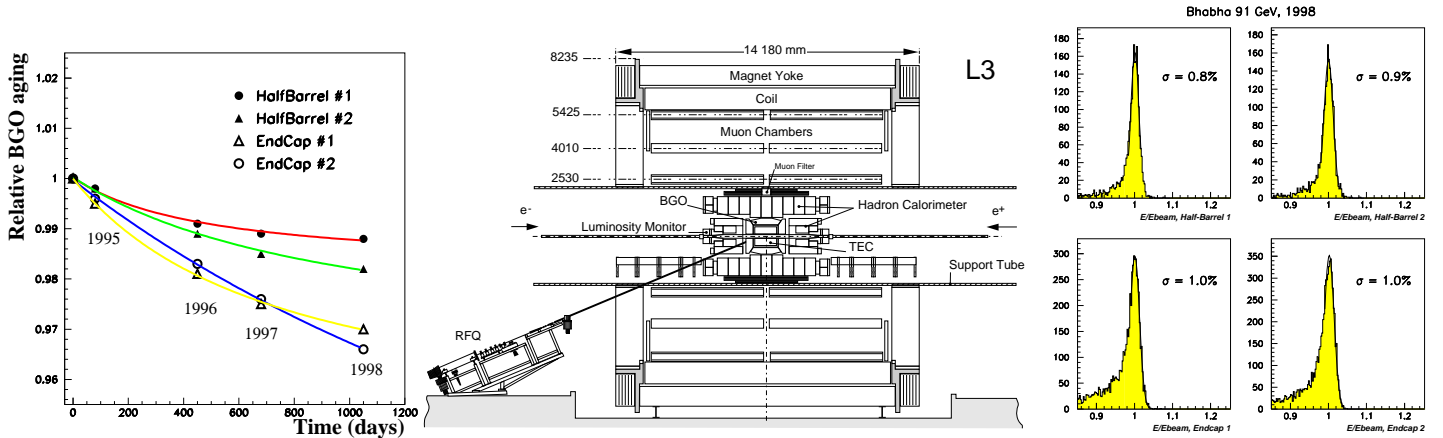


FIG. 3. Left: BGO aging at LEP. Middle: Layout of the L3-RFQ calibration system. Right: L3 Bhabha peaks obtained with RFQ calibration.

#### IV. RADIATION DAMAGE IN SCINTILLATING CRYSTALS

All known crystal scintillators suffer from radiation damage. The most common damage phenomenon is the appearance of radiation-induced absorption bands caused by color center formation. Absorption bands reduce crystal's light attenuation length (LAL), and hence the light output. Color center formation, however, may or may not cause a degradation of the light response uniformity. Radiation also causes phosphorescence (afterglow), which leads to an increase of readout noise. Additional effect may include a reduced intrinsic scintillation light yield (damage of scintillation mechanism), which would lead to a reduced light output and a deformation of the light response uniformity. Damage may recover under room temperature, which leads to a so called “dose rate dependence”. Finally, thermal annealing and optical bleaching may be effective in eliminating color centers in crystals. Reference [9] and the references therein provide detailed information for readers with interest. Because of limited scope we only highlight two points below.

First, scintillation mechanism in scintillating crystals is usually not damaged by radiation. Degradation of light output is thus due only to radiation-induced absorption, i.e. color center formation. As a consequence, irradiation does not change light response uniformity. Figure 4 shows light response uniformity as a function of accumulated dose for full size CsI(Tl) (left) and PbWO<sub>4</sub> (right) crystals. Pulse heights measured in nine points evenly distributed along the longitudinal axis of the crystal is fit to Equation 1, showing clearly that the slope ( $\delta$ ) does not change up to 10 krad for a CsI(Tl) sample, even only the front few cm of the sample was irradiated [10], and to 2.2 Mrad for a PbWO<sub>4</sub> sample [11]. This result is understood, as the intensity of all light rays attenuates equally after passing the same radiation-induced absorption zone in the crystal. A ray-tracing simulation shows that the slope of light response uniformity depends only on crystal geometry for crystals with long enough light attenuation length, and will change only if light attenuation length degrades to less than about 4 times crystal length [9]. This leads to a conclusion that crystal's energy resolution would not degrade by radiation although its calibration does change, which was confirmed by beam test at CERN [4]. Since degradation of the amplitude of light output can be inter-calibrated with physics events, or by a light monitoring system if it is caused by optical absorption, crystal precision can be maintained *in situ* even radiation damage does occur.

Second, the level of light output degradation under continuous irradiation of certain dose rate approaches an equilibrium, leading to a dose rate dependent damage, which was also later confirmed in CERN beam test [12]. This “dose rate dependence” of light output degradation is understood to be caused by color center kinetics of the creation and annihilation of radiation induced color centers [11,9].

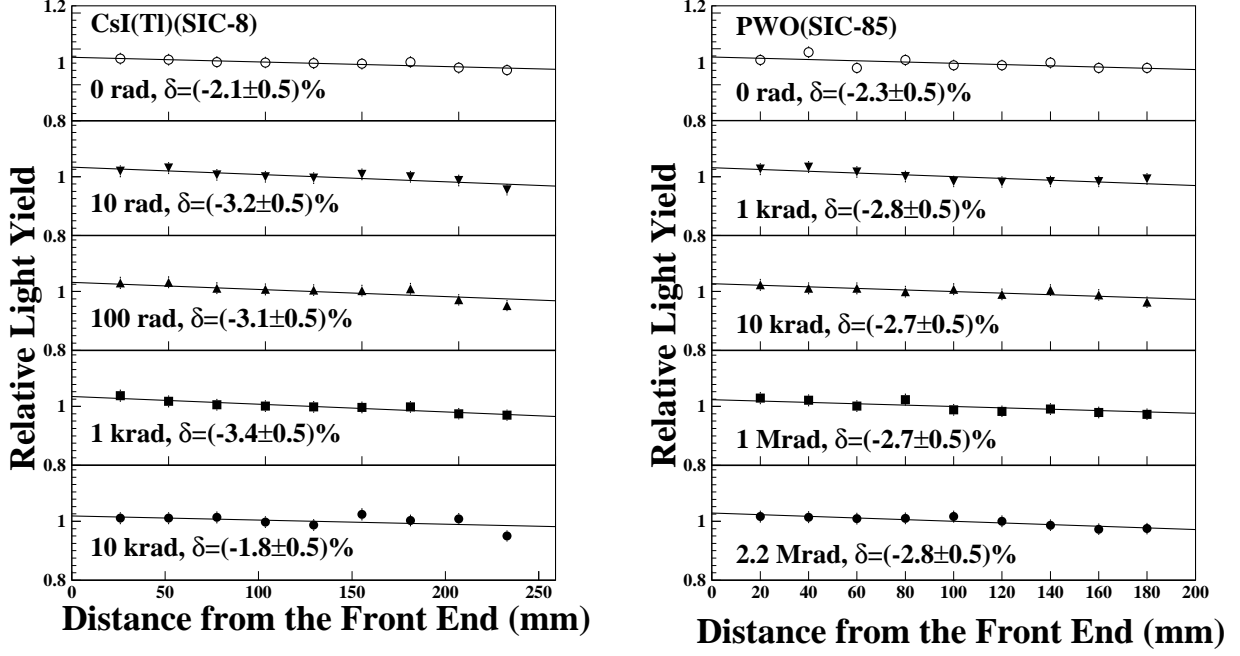


FIG. 4. Light response uniformities are shown as a function of integrated dose for full size CsI(Tl) [10] (left) and PbWO<sub>4</sub> [11] (right) samples.

If both annihilation and creation coexist, the color center density at the equilibrium depends on the dose rate applied. Assuming annihilation speed of a color center  $i$  is proportional to a constant  $a_i$  and its creation speed is proportional to a constant  $b_i$  and dose rate ( $R$ ), the differential change of color center density when both processes coexist can be written as [13]:

$$dD = \sum_{i=1}^n \{-a_i D_i + (D_i^{all} - D_i) b_i R\} dt, \quad (3)$$

where  $D_i$  is the density of the color center  $i$  in the crystal and the summation goes through all centers. The solution of Equation 3 is

$$D = \sum_{i=1}^n \left\{ \frac{b_i R D_i^{all}}{a_i + b_i R} [1 - e^{-(a_i + b_i R)t}] + D_i^0 e^{-(a_i + b_i R)t} \right\}, \quad (4)$$

where  $D_i^{all}$  is the total density of the trap related to the center  $i$  and  $D_i^0$  is its initial density. The color center density in equilibrium ( $D_{eq}$ ) thus depends on the dose rate ( $R$ ).

$$D_{eq} = \sum_{i=1}^n \frac{b_i R D_i^{all}}{a_i + b_i R}, \quad (5)$$

By using color center kinetics, one can calculate, or predict, crystal damage at one dose rate by using data collected at another dose rate [14].

## V. DAMAGE MECHANISM IN SCINTILLATING CRYSTALS

Understanding damage mechanism in scintillators would help to improve quality of mass produced crystals, which is usually achieved by material analysis. Glow Discharge Mass Spectroscopy (GDMS) analysis was tried in Charles Evans & Associates and Shiva Technology, looking for correlations between the trace impurities in crystals and their

radiation hardness. Samples were taken 3 to 5 mm below the surface of the crystal to avoid surface contamination. For both CsI(Tl) and PbWO<sub>4</sub> crystals, a survey of 76 elements, including all of the lanthanides, indicates that there are no obvious correlations between the detected trace impurities and crystal's susceptibility to the radiation damage. This indicates possible role of other defects, such as oxygen contamination or stoichiometric vacancies, which can not be determined by GDMS.

### A. Damage Mechanism in Alkali Halides

Oxygen contamination is known to cause radiation damage in alkali halide scintillators. In BaF<sub>2</sub> [2], for example, hydroxyl (OH<sup>-</sup>) may be introduced into crystal through a hydrolysis process, and latter decomposed to interstitial and substitutional centers by radiation through a radiolysis process. Equation 6 shows a scenario of this process:



where subscript *i* and *s* refer to interstitial and substitutional centers respectively. Both O<sub>s</sub><sup>-</sup> and U (H<sub>s</sub><sup>-</sup>) centers were identified [2].

Following BaF<sub>2</sub> experience, effort was made to remove oxygen contamination in CsI(Tl) crystals. A scavenger was used at SIC to remove oxygen contamination, leading to significant improvement of CsI(Tl) quality [10]. The left side of Figure 5 shows the light output as a function of accumulated dose for full size CsI(Tl) samples, compared to the *BaBar* radiation hardness specification (solid line). While the late samples SIC-5, 6, 7 and 8 (with scavenger) satisfy the *BaBar* specification, early samples SIC-2 and 4 did not. The function of the scavenger is to form oxide with density less than CsI, so will migrate to the top of ingot during growing process, similar to zone-refining. By doing so, both oxygen and scavenger are removed from the crystal.

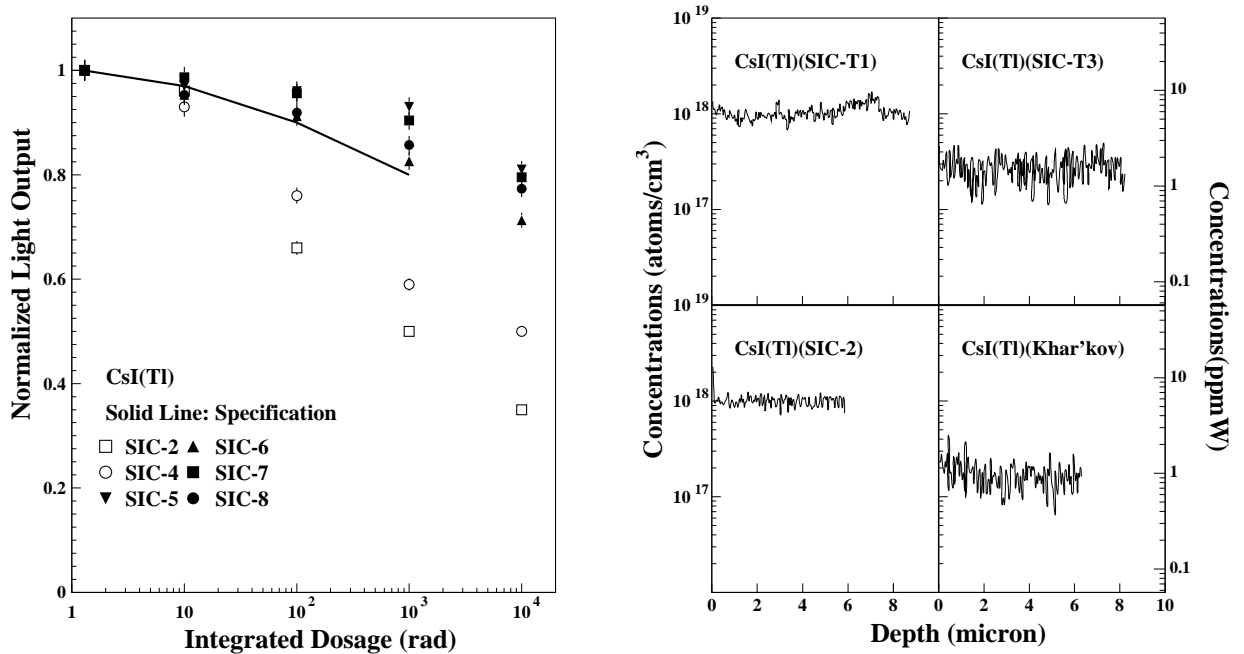


FIG. 5. Left: The progress of CsI(Tl) radiation hardness is shown for full size (~30 cm) CsI(Tl) samples from SIC together with the rad-hard specification of *BaBar* experiment. Right: Right: The depth profiles of oxygen in CsI(Tl) samples measured at Charles Evans & Associates by using SIMS analysis.

Quantitative identification of oxygen contamination in CsI(Tl) samples needs additional analysis. Gas Fusion (LECO) at Shiva Technologies West, Inc., found that oxygen contamination in all CsI(Tl) samples is below detection

limit of 50 ppm. Secondary Ionization Mass Spectroscopy (SIMS) was tried at Charles Evans & Associates. A Cs ion beam of 6 keV and 50 nA was used to bombard the CsI(Tl) sample. All samples were freshly cleaved prior before being loaded to the UHV chamber. An area of  $0.15 \times 0.15 \text{ mm}^2$  on the cleaved surface was analyzed. To further avoid surface contamination, the starting point of the analysis is at about  $10 \mu\text{m}$  deep inside the fresh cleaved surface. The right side of Figure 5 shows depth profile of oxygen contamination for two rad-soft (SIC-T1 and SIC-2) and two rad-hard (SIC-T3 and Khar'kov) CsI(Tl) samples. Crystals with poor radiation resistance have oxygen contamination of  $10^{18} \text{ atoms/cm}^3$  or 5.7 ppmW, which is 5 times higher than the background count ( $2 \times 10^{17} \text{ atoms/cm}^3$ , or 1.4 ppmw). The radiation damage in CsI(Tl) is indeed caused by oxygen contamination.

### B. Damage Mechanism in Oxides

Crystal defects, such as oxygen vacancies, is known to cause radiation damage in oxide scintillators. In BGO, for example, three common radiation induced absorption bands at 2.3, 3.0 and 3.8 eV were found in a series of 24 doped samples [15], indicating defect-related color centers, such as oxygen vacancies. Following the BGO experience, an effort was made at SIC to reduce oxygen vacancies in  $\text{PbWO}_4$  crystals by oxygen compensation through post-growth thermal annealing in an oxygen-rich atmosphere, and result was positive [11].

Particle Induced X-ray Emission (PIXE) and quantitative wavelength dispersive Electron Micro-Probe Analysis (EMPA) was tried in Charles Evans & Associates to quantify stoichiometry deviation and oxygen vacancies in  $\text{PbWO}_4$  crystals. Crystals with poor radiation hardness were indeed found to have a non-stoichiometric W/Pb ratio [11]. However, both PIXE and EMPA did not provide oxygen analysis. X-ray Photoelectron Spectroscopy (XPS) at Charles Evens & Associates was found to be very difficult to reach a stable quantitative conclusion because of large systematic uncertainties in oxygen analysis [16].

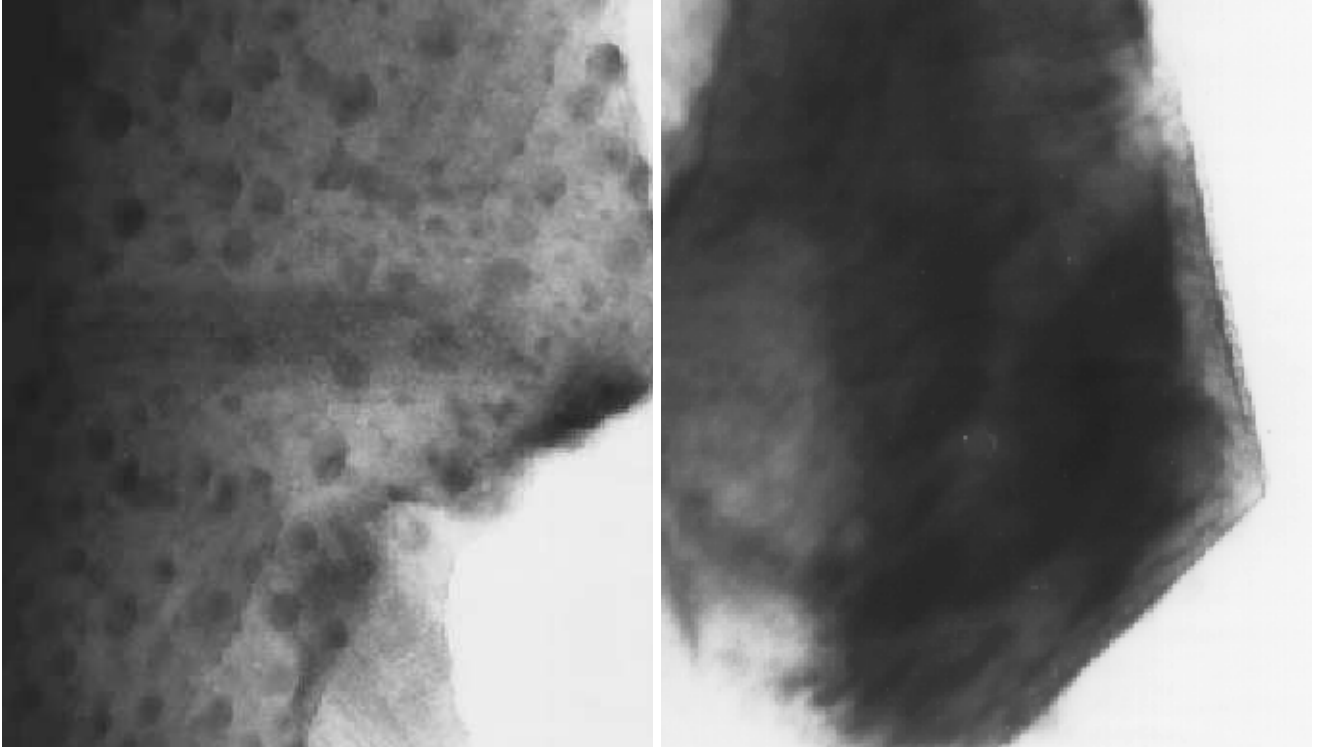


FIG. 6. TEM pictures of a  $\text{PbWO}_4$  crystal of poor (left) radiation hardness, showing clearly the black spots of  $\phi 5\text{--}10 \text{ nm}$  related to oxygen vacancies, as compared to that of a good one (right).

By using Transmission Electron Microscopy (TEM) a localized stoichiometry analysis was possible to identify oxygen vacancies. A TOPCON-002B Scope was first used at 200 kV and 10  $\mu$ A. Samples were made to powders of an average grain size of a few  $\mu$ m, and then placed on a sustaining membrane. Figure 6 shows TEM pictures taken for a pair of samples of poor (left) and good (right) radiation hardness. Black spots of a diameter of 5 – 10 nm were clearly observed in the poor sample, but not in the good sample. These black spots were identified as regions with severe oxygen deficit by a localized stoichiometry analysis using TEM coupled to Energy Dispersion Spectrometry (EDS) [17]. Approaches to reduce oxygen deficits were taken by crystal vendors, leading to production crystals of much improved quality.

## VI. SUMMARY

Precision crystal calorimetry extends physics reach in experimental high energy physics because of its best achievable resolution for electrons and photons. An optimized light response uniformity is the key to reach crystal energy resolution. A precision calibration is the key to maintain crystal precision *in situ*.

Predominant radiation damage effect in crystal scintillators is radiation induced absorption, or color center formation, not damage of scintillation mechanism. For precision calorimetry, crystal scintillator must preserve its light response uniformity under irradiation, which requires a long enough initial light attenuation length and a low enough radiation induced color center density. A precision light monitoring may function as inter-calibration for such crystals.

Radiation damage in alkali halides is caused by oxygen and/or hydroxyl contamination, as evidenced by a SIMS analysis and the effectiveness of a scavenger in removing oxygen contamination in CsI(Tl) crystals. Radiation damage in oxides is caused by stoichiometry-related defects, e.g. oxygen vacancies, as evidenced by a localized stoichiometry analysis using TEM/EDS, and the effectiveness of the oxygen compensation for PbWO<sub>4</sub> crystals.

## ACKNOWLEDGEMENTS

Measurements at Caltech were carried out by Mr. Q. Deng, H Wu, D.A. Ma, Z.Y. Wei and T.Q. Zhou. Part of the PbWO<sub>4</sub> related work was carried out by Dr. C. Woody and his group at Brookhaven National Laboratory.

- 
- [1] G. Gratta *et al.*, *Annu. Rev. Nucl. Part. Sci.* **44** 453 (1994).
  - [2] R.Y. Zhu, *Nucl. Instr. and Meth.* **A340** 442 (1994).
  - [3] D. Graham and C. Seez, *CMS Note* **1996/002**.
  - [4] E. Auffray *et al.*, *Nucl. Instr. and Meth.* **A412** 223 (1998); and G. Alexeev *et al.*, *Nucl. Instr. and Meth.* **A385** 425 (1997).
  - [5] *The CMS Electromagnetic Calorimeter Project*, CERN/LHCC **97-33** (1997).
  - [6] U. Chaturvedi *et al.*, will be published in *IEEE Trans. Nucl. Sci.* **NS-46**.
  - [7] L3 Collaboration, *Nucl. Instr. and Meth.* **A289** 35 (1990).
  - [8] E. Cheu *et al.*, “*Proposal to Continue the Study of Direct CP Violation and Rare Decay Process in KTeV in 1999*”, December (1997).
  - [9] R.Y. Zhu, *Nucl. Instr. and Meth.* **A413** 297 (1998).
  - [10] R.Y. Zhu *et al.*, in *Proc. of the 6th Int. Conf. on Calorimetry in High Energy Physics*, ed. A. Antonelli *et al.*, Frascati Physics Series 589 (1996).
  - [11] R.Y. Zhu *et al.*, *Nucl. Instr. and Meth.* **A376** 319 (1996), *IEEE Trans. Nucl. Sci.* **NS-44** 468 (1997), **NS-45** 668 (1998).
  - [12] C. Seez, *CMS Internal Note* **1998/026**.
  - [13] D.A. Ma *et al.*, *Nucl. Instr. and Meth.* **A332** 113 (1993) and *Nucl. Instr. and Meth.* **A356** 309 (1995).
  - [14] Q. Deng *et al.*, *CMS Note* **1998/083**, to be published in *Nucl. Instr. and Meth.*.
  - [15] R.Y. Zhu *et al.*, *Nucl. Instr. and Meth.* **A302** 69 (1991),
  - [16] C. Lazik of Charles Evans and Associates, private communications.
  - [17] Z.W. Yin *et al.*, in *Proceedings of SCINT97 Int'l Conf.*, ed. Z.W. Yin *et al.*, CAS Press 191 (1997).